

RESEARCH ARTICLE

Investigating and Modeling Ageing Effects on Polymeric Insulator Electrical Properties

ALI AHMED SALEM^{1,2}, (Member, IEEE), AHMED ALLAWY ALAWADY^{3,4},
 KWAN YIEW LAU⁵, (Senior Member, IEEE), WAN RAHIMAN^{6,7,8}, (Member, IEEE),
 ZULKURNAIN ABDUL-MALEK⁹, (Senior Member, IEEE),
 SAMIR AHMED AL-GAILANI^{5,9}, SALEM MGAMMAL AL-AMERI¹⁰,
 ENAS ALI¹¹, AND SHERIF S. M. GHONEIM¹², (Senior Member, IEEE)

¹School of Electrical Engineering, Universiti Teknologi MARA, Shah Alam 40450, Malaysia

²School of Electrical Engineering, Sana'a University, Sana'a, Yemen

³Computer Technique Engineering Department, College of Technical Engineering, The Islamic University, Najaf 54001, Iraq

⁴Medical Laboratory Techniques Department, Alamal College For Specialized Medical Sciences, Karbala 56001, Iraq

⁵Institute of High Voltage and High Current, School of Electrical Engineering, Universiti Teknologi Malaysia, Johor Bahru 81310, Malaysia

⁶School of Electrical and Electronic Engineering, Universiti Sains Malaysia, Engineering Campus, Nibong Tebal, Penang 14300, Malaysia

⁷Cluster of Smart Port and Logistic Technology (COSPALT), Universiti Sains Malaysia, Engineering Campus, Nibong Tebal, Penang 14300, Malaysia

⁸Daffodil Robotics Laboratory, Department of Computer Science and Engineering, Daffodil International University, Dhaka 1216, Bangladesh

⁹Faculty of Engineering and Computer Technology, AIMST University, Bedong, Kedah 08100, Malaysia

¹⁰Department of Electrical and Computer Engineering, Curtin University Malaysia, Miri 98009, Malaysia

¹¹Faculty of Engineering and Technology, Future University in Egypt, New Cairo 11835, Egypt

¹²Department of Electrical Engineering, College of Engineering, Taif University, Taif 21944, Saudi Arabia

Corresponding authors: Ali Ahmed Salem (en.alisalem@gmail.com) and Wan Rahiman (wanrahiman@usm.my)

This work was supported in part by Universiti Sains Malaysia through Bridging GRA under Grant 304/PELECT/6316603; in part by the Universiti Teknologi MARA (UiTM) Shah Alam; in part by Universiti Teknologi Malaysia Fundamental Research under Grant 22H34; and in part by the Deanship of Scientific Research, Taif University.

ABSTRACT Polymeric insulators, in particular silicone rubber (SIR) are lightweight, have good hydrophobicity characteristics, and are easy to carry and install. They are commonly used for outdoor insulation in power lines. However, pollution, UV radiation, temperature, discharge, wetness, and stress can cause them to degrade over time, losing their electrical properties. Therefore, evaluating the ageing and degradation of polymeric insulators under different conditions becomes crucial. This paper investigates the ageing effects of the polymeric insulators with differences in pollution, applied voltage, hydrophobicity class, and geometrical structures of insulators. The investigation includes the experimental tests of the insulators' electrical properties such as leakage current and flashover voltage, after assessing the initial characteristics of insulators based on their age and supply voltage. In addition, the aged polymeric insulator model based on an equivalent circuit model was developed to determine the leakage current and breakdown voltage of aged insulators. Moreover, an artificial neural network model is carried out to predict the critical leakage current and flashover voltage of the insulator under the ageing effect. The experiment results were used to validate the accuracy of the proposed models; with an aggregate error of less than 10%, the proposed models appeared to be satisfactory. These models can serve as a scholarly resource for designing, operating, and maintaining insulators, especially in polluted environments.

INDEX TERMS Polymeric insulator, leakage current, pollution, insulator ageing, geometrical characteristics.

I. INTRODUCTION

The global growth in electrical energy consumption has created a slew of technological issues in ensuring the

The associate editor coordinating the review of this manuscript and approving it for publication was S. Sofana Reka .

dependability of electrical distribution and transmission systems. Some of the most important aspects are the proper design and operation of the components involved in the different systems, including insulators. Insulators play a significant role in the dependability of power systems as an integral part of transmission power lines, and their failure puts the

power systems at risk [1], [2], [3], [4], [5]. Glass and ceramic materials are often used to make electrical insulators. However, harsh weather conditions and pollution can impair their efficiency; as a result, polymeric insulators offer an effective alternative for developing more reliable electrical systems [5], [6]. Polymeric insulators offer various advantages compared to traditional insulators, including its hydrophobic surface, lightweight, and resistance to vandalism and contamination flashover [8], [9]. The main justification for choosing polymeric insulators is their performance in contaminated environments.

Unlike ceramic insulators, whose physical and chemical characteristics do not alter noticeably over time, polymeric materials' characteristics vary significantly with ageing. Ageing is the term used to describe the degradation of polymeric materials brought on by electrical and environmental stresses [9], [10]. Ultraviolet (UV) radiation, temperature, moisture, and contaminations are examples of environmental stresses [10], [11]. As polymeric materials age, they lose some of their hydrophobicity, which causes the insulator surface to become moist more quickly [11], [12]. In the presence of contamination and humidity, this will result in an increase in electrical conductivity and an increase in leakage current. Subsequently, dry band development on the insulator surface becomes stronger, dry band discharges rise, and the leakage current (LC) waveform becomes more distorted [13], [14].

To date, few studies have investigated the performance of aged polymeric insulators with respect to LC. In [16], the LC was used to predict flashover voltage. The above study is limited to LC performance as a parameter of the prediction model. However, the LC is a good indicator to evaluate the insulators situation under different initial or external factors such as contamination, age, hydrophobicity class (HC) and geometric of insulators. Researchers have looked closely at the properties of polymeric insulators in various environmental settings, including LC. The LC has been used to study environmental stresses such as pollution, humidity, temperature, ageing, and hydrophobicity of polymeric insulators [17], [18], [19], [20], [21], [22]. In [17], the LC characteristics/indicators have been extracted to estimate the condition of polymeric insulators. The findings demonstrated that each indicator provided was helpful for assessing the state of contaminated insulators. Authors in [19] have presented a comprehensive analysis of silicone rubber insulator's LC under different pollution, humidity, and ageing conditions. They reported that the LC increased significantly during the dry band arcing and corona discharges conditions. The flashover voltage occurrence on polymeric insulators under variation in pollution and humidity has been predicted using LC harmonic components criteria [22]. However, the study predicted the flashover voltage of composite insulators based on environmental conditions and ignored the chemical conditions.

The parameters related to geometrical form influence the contamination performance of insulators, where leakage

distance plays a crucial role. The shape factor of the insulator, its height, and diameter are important factors affecting flashover performance [23]. In [16], experiments were conducted to predict the flashover voltage of two different profiles of composite insulators under various pollution levels and hydrophobicity classes, using flashover voltage and LC tests, where the components of LC were used as input for artificial neural network (ANN) model. Authors in [24] stated that the analysis of the LC of insulators aided in the assessment of high-voltage insulator conditions. According to research in [25], [26], and [27], evaluating insulators can benefit from using the empirical fitting formula of the impact of pollutants on flashover performance. Accordingly, this study used an empirical fitting method for developing the model of LC of polymer insulators.

Prior research has investigated the influence of pollution on insulators based on LC. However, there remains a gap in knowledge concerning a thorough comprehension of insulator LC based on its electrical parameters.

In this study, experimental tests on suspension polymeric insulators with varying geometries to evaluate the ageing effects on their electrical characteristics. After measuring the initials characteristics of insulators, they have been investigated under artificial conditions, including contamination, hydrophobicity, applied voltage, and geometrical parameters of insulator structures. The equivalent circuit model is employed to determine the critical LC with respect to pollution levels. Furthermore, An ANN model is designed to predict the electrical properties based on pollution severity, ageing, hydrophobicity level, applied voltage, and insulator dimensions. Finally, the models are compared to the test data, and their performances are evaluated using root mean square error (RMSE), mean squared error (MSE), coefficient of determination (R^2), and absolute average deviation (AAD).

The remainder of the paper is organized as follows: section II describes the experimental works of LC Section III discusses the experimental work results. Section IV describes in detail the proposed model and related improved modules, and then compares the model result to the test results. Section V is the conclusion.

II. EXPERIMENTAL SETUP

A. TEST SAMPLE

Three 33 kV silicone rubber polymeric insulators with three different geometries were selected for this study, as shown in Figure 1. Each selected insulator, with three samples having three different ageing periods were selected, which resulted in three different HC.

The insulators' geometric specifications are listed in Table 1. Among them, S denotes the spacing between the sheds, D and d stand for the diameters of the big and small sheds, respectively, L indicates the leakage distance, H is the height of the insulator, and L/H signifies the creepage factor. The HC for each age class was listed in Table 2 along with

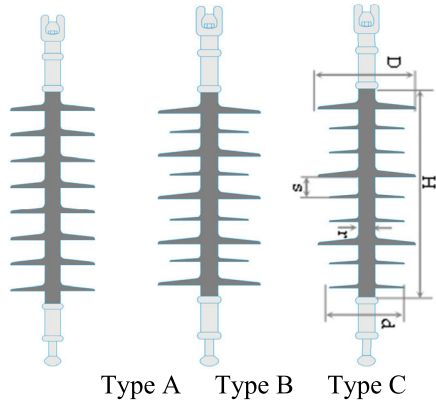


FIGURE 1. Insulators' structure diagram.

TABLE 1. Structure parameters of test composites insulators.

Parameters	Insulator type		
	A	B	C
Voltage operation, $V(kV)$	33	33	33
Hight, H (cm)	39	41	48.3
Leakage distance, L (cm)	93	131	160
Small, shed diameter, d (cm)	-	9	9
Large, shed diameter, D (cm)	9.8	13	13
Trunk diameter, r (cm)	3	3	3
Trunk distance, s (cm)	4.5	4.1	4.6
Equivalent diameter D_{eq} (cm)	5.95	7	8.3
No. of sheds(large/small)	8/-	5/4	3/6
Form factor	5.34	5.46	5.53

TABLE 2. Ages and Hydrophobicity class of the selected insulators.

Parameters	Classes		
	#1	#2	#3
Operation years	New (0)	7	15
Hydrophobicity Class	HC1	HC3	HC5

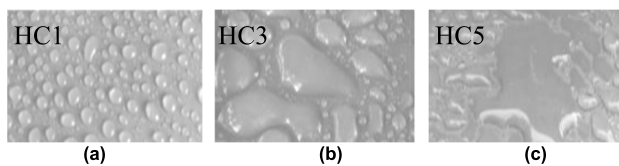


FIGURE 2. Hydrophobicity classes: (a) HC1; (b) HC3; (c) HC5.

the age of the tested insulators. The insulators surface cross pending the selection HC were shown in figure 2.

B. EXPERIMENTAL PROCEDURE AND SAMPLE PREPARATION

Figure 3 shows the circuit diagram and Laboratory view of LC and voltage test of SiR insulators. An AC step-up transformer of 240V/250 kV is used to energise the samples under test. To simulate the environmental test, the samples were tested in the test chamber made up of polycarbonate walls with dimensions of 120 cm width, 120 lengths and 175 cm height. Following preparation, the insulator was suspended vertically in the test room and its bottom side was

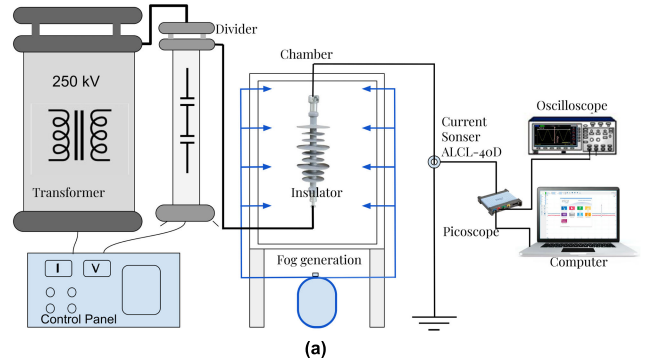


FIGURE 3. Experimental setup. (a) Block diagram;(b) Laboratory view.

connected to an AC source while the top side was grounded. Additionally attached to the transformer was a capacitive divider, which was used to measure the insulator's input voltage. LC was measured using an effective current sensor ALCL-40D clamped on the ground wire. The current sensor measurement range of 10^{-3} to 50 mA, and its accuracy was evaluated around 0.2% for a 2 mA. The voltage and current output signals were captured concurrently on the digital oscilloscope and computer. To wet the insulator's surface, the fog generator was used to supply the test room with fog. Eight fog inters were installed at the chamber wall to distribute the fog uniformly and cover the whole room, completely wetting the surface of the entire test sample.

To create the artificial contamination layer on the surface of the insulators, The insulator was cleaned and left to dry naturally. The solid layer method [28], [29], which has been utilized in accordance with IEC 60507 [30] to imitate the contamination state of the insulators in service, was adopted. To create an artificial pollution layer with varying conductance levels, varying weights of soluble salts were mixed with kaolin in 500 mg deionized water. In this paper, three pollution levels represented by equivalent salt deposit densities (ESDD) were set to 0.05, 0.15, and 0.25 $mg.cm^{-2}$. The ratio of non-soluble deposit density NSDD to ESDD has been set at a constant value of 4 in all tests. It is worth noting that the ESDD were simulated by sodium chloride salt (NaCl).

The surface of the insulator was sprayed with a solution mixed with distilled water, salt, and kaolin. Before spraying, a thin film of kaolin powder was applied to the insulator's surface to temporarily reduce hydrophobicity and create a homogenous layer of contamination. After being sprayed with the contamination solution, the insulators were left to dry for 24 hours in a natural environment. The insulator was cleaned once again with distilled water to determine the contamination level by calculating the ESDD and NSDD using the following formula [31]:

$$S_a = (0.57\sigma_{20})^{1.03} \text{ mg/cm}^3 \quad (1)$$

$$ESDD = \frac{S_a \times V}{A} \text{ mg/cm}^2 \quad (2)$$

$$NSDD = \frac{W_f - W_i}{A} \text{ mg/cm}^2 \quad (3)$$

where S_a represents the salinity, σ_{20} is solution conductivity at 20 °C, V is the distilled water volume, A is the insulator surface area for collecting pollutants and W_i and W_f are the initial weight of the filter paper in dry conditions and the weight of the filter paper containing pollutants, respectively. The insulator was then installed in the fog chamber. The contaminated insulator was wetted with a fog flow rate of 5 L/h, which is adequate to reach maximal conductance of the pollution layer between 20 and 50 minutes depending on the tested insulator [32]. After the sample contamination stage was complete, the specimen was introduced into the test chamber to start the test. The wetting procedure was performed before the testing of the insulator. The specimen was saturated with moisture before the voltage was applied. The surface hydrophobicity of each insulator was measured and analyzed using a technique according to the Swedish transmission research Institute STRI [33]. The STRI process is spraying tap water for 20 seconds and collecting photos with a high-resolution camera within 10 seconds of the spray.

The LC, conductance of the samples was monitored under operation voltage of 33kV under various conditions.

C. ELECTRICAL CHARACTERISTICS MEASUREMENT

The insulator was suspended, the experiment circuit was connected, and the applied voltage was increased to the operating voltage value of the insulator. The up and down technique was used to control the applied voltage. The step voltage was set to be 3 kV. The electrical parameters like flashover voltage, current, and output voltage were measured five times at 10 minutes intervals to avoid measurement error. The electrical characteristics were measured under three applied voltage levels: 25 kV, 30 kV and 35 kV, except in the case of high pollution, where the insulators flashover may occur before reaching 25 kV. From the output signals of current and voltage, the root mean square values (RMS) of LC and voltage was calculated using Equation (4):

$$RMS = \sqrt{\frac{1}{n} \sum_i x_i^2} \quad (4)$$

where n is the number of measurements and x_i represents the measurement value at i . The average flashover voltage and standard deviation error SD (%) were determine using equations (5) and (6) as [34], [35]:

$$U_a = \frac{\sum (U_i n_i)}{N} \quad (5)$$

$$\sigma\% = \sqrt{\left(\frac{\sum_{i=1}^N (U_i - U_a)^2}{(N - 1)} \right) / (100/U_a)} \quad (6)$$

where U_i is the source voltage, n_i is number of tests performed at U_i and N is number of total tests. As previously mentioned, the LC signal was monitored simultaneously throughout the test using the current sensor ALCL-40D. Then, by dividing the amplitudes of the voltage source by the amplitude of the LC, the resistance of the contaminated layer was estimated. When the input voltage is raised, the electric field causes water droplets to lengthen and come together to form conducive passes, which results in a decrease in the resistance of insulator surface. In each step of applied voltage, the LC was measured, and the conductance of insulator surface was deduced according to Ohm's law in Equation (7),

$$G = \frac{I_o}{U_i} \quad (7)$$

where I_o is the measured LC and U_i is the applied voltage. To calculate the pollution layer resistance in the presence of electrical discharge, the equivalent circuit of polluted insulator has been modeled. The detailed polluted insulator model will be discussed in the next section.

III. EXPERIMENTAL RESULTS

This section is layout by subheadings. The electrical characteristics and hydrophobicity corresponding to sample ageing were investigated. The model parameters proposed for three sample insulators are presented, along with the recorded LC waveforms during the high-voltage test. Next, the performance of insulator conductance under different conditions was presented. Finally, the experimental results will be compared to the output of the proposed model.

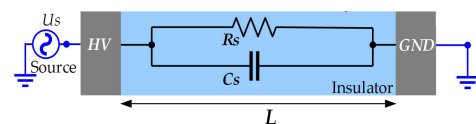


FIGURE 4. Insulator model.

A. INITIAL ELECTRICAL CHARACTERISTICS OF INSULATORS

Figure 4 shows a clean insulator made up of resistance (R_s) in parallel with capacitance (C_s). The initial electrical characteristics of a polymeric insulator represent the resistance, conductance, dissipation factor (DDF, also known as $\tan \delta$) and LC. In the beginning, in order to calculate the C_s of the tested insulators, the $\tan \delta$ was measured.

By measuring the LC of insulators under dry and clean conditions, the capacitance C_s of the insulators were calculated using Equation (8).

$$C_s = \frac{I_{peak} \sin \theta}{2\pi f V_{peak}} \quad (8)$$

where I_{peak} and V_{peak} are the peak amplitude of LC and applied voltage, respectively. θ represents the phase shift angle between the LC and applied voltage. f denotes the system frequency, which is 50 Hz. To extract I_{peak} and θ from the signal of current, the fast Fourier transform (FFT) was applied to the LC waveform in time domain. In order to calculate the insulator's resistance, the insulator's dissipation factor ($\tan \delta$), which given by the Equation (9), has been measured.

$$\tan \delta = \frac{I_R}{I_C} = \frac{U \cdot G_s}{U \cdot 2\pi f C_s} = \frac{G_s}{\omega C_s} \quad (9)$$

where $G_s = 1/R_s$ is conductance of insulator material. From (9), the insulator's conductance G_s can be calculated as,

$$G_s = \omega C_s \times \tan \delta \quad (10)$$

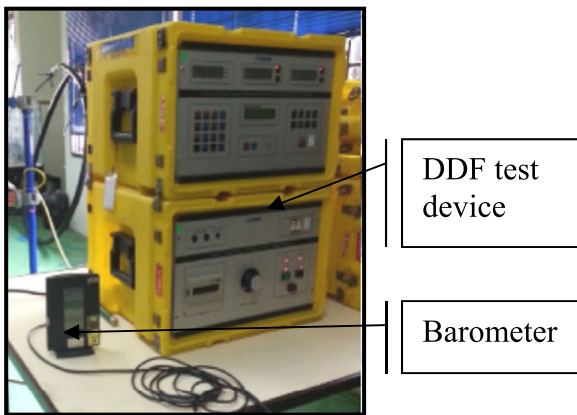


FIGURE 5. $\tan \delta$ measurement device (DDF-test).

The insulator DDF ($\tan \delta$) was measured directly using the fully automatic capacitance precision measuring bridge type 2816a shown in Figure 5.

Figure 6 shows the $\tan \delta$ values of insulators under different ages and three levels of voltages. As can be seen in Figure 5, the $\tan \delta$ value is unique for each insulator, suggesting that each insulator has different qualities and properties due to variations in the resistance of the lossy part, which are caused by ageing. As the insulator age increases, the value of $\tan \delta$ also increases. This increase in $\tan \delta$ indicates that the quality of the insulation is progressively decreasing. Insulator B can be considered a good insulator because it has a low $\tan \delta$ value, as indicated by the measurement.

Table 3 shows the results of calculating the internal capacitance and conductance (C_s and G_s) of the measured polymer insulators, using the peak amplitude of the

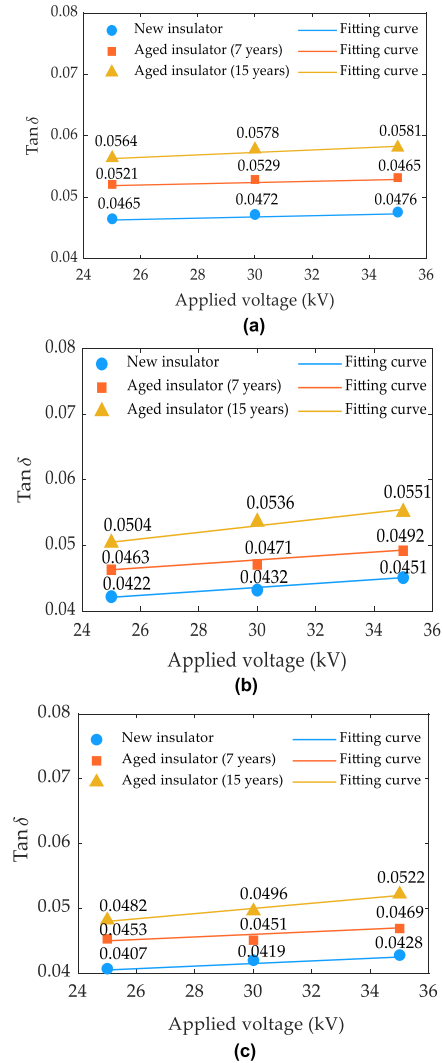


FIGURE 6. Dielectric dissipation factor, $\tan \delta$, of (a) insulator A; (b) insulator B; (c) insulator C.

leakage current (I_{peak}), the peak amplitude of the applied voltage (V_{peak}), the phase difference between them (θ) and $\tan \delta$. These parameters were calculated using equations (8) and (10). As shown in Table 4, ageing in insulators causes:

- 1) The observed values of LC, dissipation factor ($\tan \delta$), and calculated insulator capacitance increased as the polymer aged. The increase in capacitance C_s is owing to the formation of polar molecules such as carboxyl and hydroxyl, as well as the penetration of water polar molecules in the polymer. Polarization currents are formed because of these polar substances. This polarization implies electrical energy storage, resulting in a modest increase in capacitance C_s .
- 2) The insulator conductance has increased. This is because of the polarization phenomenon, which leads to the rise of the dissipation under AC voltage, and hence \tan and G_s increase.

TABLE 3. The electrical characteristics of insulators.

Insulator	Age	V (kV)	I (mA)	θ	C_s (PF)	G_s (μ S)	
A	0	25	0.016	77.63	1.988	2.905	
		30	0.023	76.53	2.373	3.519	
		35	0.036	76.21	3.179	4.665	
	7	25	0.018	76.65	2.232	3.652	
		30	0.027	76.19	2.782	4.623	
		35	0.039	75.68	3.437	5.895	
	15	25	0.021	76.06	2.595	4.598	
		30	0.031	75.53	3.185	5.783	
		35	0.042	75.72	3.702	6.757	
	B	0	25	0.014	79.35	1.752	2.322
			30	0.025	78.59	2.082	2.823
			35	0.026	77.98	2.313	3.277
7		25	0.017	78.32	2.126	3.083	
		30	0.023	77.92	2.386	3.531	
		35	0.033	77.62	2.931	4.531	
15		25	0.022	77.89	2.739	4.336	
		30	0.038	77.55	3.108	5.234	
		35	0.037	77.02	3.279	5.676	
C		0	25	0.012	82.47	1.515	1.937
			30	0.015	81.93	1.576	2.074
			35	0.019	81.32	1.708	2.297
	7	25	0.015	81.25	1.888	2.686	
		30	0.021	80.71	2.199	3.116	
		35	0.028	80.02	2.508	3.695	
	15	25	0.019	80.18	2.384	3.609	
		30	0.027	79.92	2.821	4.395	
		35	0.034	79.54	3.041	4.987	

B. AGE-RELATED CHANGES IN HYDROPHOBICITY

Since silicone rubber has strong hydrophobicity, it should maintain that quality as it ages. However, the hydrophobicity estimation of silicone rubber insulators before and after ageing was performed using contact angle measurement to investigate the ageing effect. Each aged test sample's contact angle was measured many times, and the mean was adopted. To determine how much the hydrophobicity had changed owing to ageing, their contact angles were measured and compared to those of fresh samples. Figure 7 displays the contact angles for each sample, both new and aged insulators under operation voltage of 33 kV.

For the new samples, the contact angles for insulator A, insulator B, and insulator C were 95.1°, 97.4°, and 95.5°, respectively. Samples were discovered to have a high hydrophobicity. Figure 6 demonstrates that insulator B has the highest value of contact angles at all age levels, indicating that it is the best.

For aged insulators, Figure 7 shows that the contact angle decreases with increasing age of sample. Take insulator A for example, by increasing the insulator age from 0, 7 and 15 years, the contact angle decreases from 95.1° to 74.8° and 58.6°, respectively. This indicates that insulator ageing under voltage supply, temperature, and humidity conditions has a significant influence on the insulator surface's loss of hydrophobicity. Therefore, the variations in contact angle showed that silicone rubber's capacity to absorb water changed because of ageing. This highlights that the investigations on the influence of ageing on the monitoring of polymeric insulators are important.

C. LEAKAGE CURRENT TEST RESULTS

The LC amplitude measured from the high voltage test results corresponding to the new and aged insulators are shown in Tables 3 to 5. The test results show an apparent ageing effect. The LC of aged insulators is higher than the LC of new insulators when ESDD is the same. The fundamental reason for this is that the layer conductivity of ageing insulators is simpler to mold on the surface. According to the test results in Tables 3 to 5, with increase of ESDD, ageing of insulators, applied voltage and HC, the LC amplitude of tested samples shows an increasing trend. Furthermore, LC amplitudes for insulator type C are the lowest when compared to insulators A and B.

1) IMPACT OF ESDD ON LC AMPLITUDE

As shown in tables 3 to 5, the LC amplitude of all insulators under test grows with increasing ESDD under a certain age, and the LC amplitude of aged insulators for 15 years increases more than that of new and old insulators for 7 years. Taking the LC of insulator A with 30 kV and HC3 as an example, with the increase of ESDD from 0.05 to 0.25 mg/cm², LC increases from 7.74 mA to 28.45 mA when the insulator is new, increasing by 268%; LC increases from 6.73 mA to 47.12 mA when the insulator's age is 7 years, increasing by 600%; LC increases from 7.63 mA to 72.07 mA when the insulator's age is 15 years, increasing by 626%. Meanwhile, with the rise of ESDD, the LC increase of insulator C is lower than that of insulator A and B under the same conditions. Taking the age of 7 years as an example, the increase of ESDD from 0.05 to 0.25 mg/cm², LC of insulator A increases as mentioned above from 6.73 mA to 47.12 mA, increasing by 600%; LC of insulator B increases from 5.56 mA to 35.33 mA, increasing by 535%; LC of insulator C increases from 4.94 mA to 32.22 mA, increasing by 552%.

The empirical formula of the relationship between LC, ESDD, and insulator's age under HC3 and applied voltage of 35 kV has been extracted by fitting the test data and can be expressed by Equation (11):

$$I = \alpha \cdot ESDD^\beta \cdot Y^\gamma \quad (11)$$

where I represents the LC, Y represents the age of the insulator, α is a coefficient related to the insulator structure, β is a characteristic exponent characterizing the impact of ESDD on LC and γ is a characteristic exponent characterizing the impact of age on LC. The fitting surfaces of LC, ESDD, and insulator age of selected insulators are illustrated in Figure 8. Equation (11) can be linearized by taking the ln of the Equation (12) as follows:

$$\ln I = \ln \alpha + \beta \cdot \ln ESDD + \gamma \cdot \ln Y \quad (12)$$

According to the least-square technique, the absolute error between the test data and the computed values according to (12) will be tiny enough if the sum of squares of deviation e is as minimal as feasible. e is written

TABLE 4. Leakage current test results in (mA) of new insulators. ESDD in (mg/cm²) and U in (kV).

HC	Type ESDD U	A			B			C		
		0.05	0.15	0.25	0.05	0.15	0.25	0.05	0.15	0.25
1	25	2.15	4.53	13.56	1.49	3.75	11.77	1.19	2.83	8.34
	30	4.85	11.25	25.94	2.93	8.51	25.35	1.72	7.21	17.42
	35	7.35	22.56	34.88	5.01	16.74	47.65	2.77	10.16	38.87
3	25	2.03	6.62	16.72	1.86	4.65	14.66	1.48	3.52	10.37
	30	5.74	17.96	28.45	3.66	10.57	22.56	2.15	8.98	21.65
	35	11.05	30.76	43.74	8.25	19.79	30.32	5.46	17.65	32.32
5	25	2.71	8.09	22.40	2.63	6.24	20.81	2.11	5.00	14.66
	30	9.75	19.74	36.85	5.21	14.94	45.77	3.06	13.03	28.37
	35	12.70	40.60	82.19	8.88	30.14	77.71	4.84	19.89	44.75

TABLE 5. Leakage current test results in (mA) of ageing insulators of 7 years. ESDD in (mg/cm²) and U in (kV).

HC	Insulator type ESDD U	A			B			C		
		0.05	0.15	0.25	0.05	0.15	0.25	0.05	0.15	0.25
1	25	2.66	7.75	17.50	2.05	6.99	16.59	2.04	6.07	15.44
	30	4.29	17.57	38.21	3.45	13.62	26.41	3.39	11.14	25.92
	35	10.84	26.25	65.79	7.64	22.03	39.07	6.00	17.59	35.95
3	25	2.89	9.26	21.58	3.31	8.68	20.66	2.56	8.81	19.19
	30	6.73	21.81	47.12	5.56	16.92	35.33	4.94	13.88	32.22
	35	14.86	39.57	60.12	9.55	27.36	43.54	7.50	22.92	37.54
5	25	3.21	13.86	28.91	4.68	11.63	29.33	3.63	12.52	27.13
	30	9.01	30.84	64.08	7.92	23.93	68.72	6.02	20.12	42.21
	35	13.95	47.23	106.7	13.56	39.68	96.34	10.49	30.99	93.18

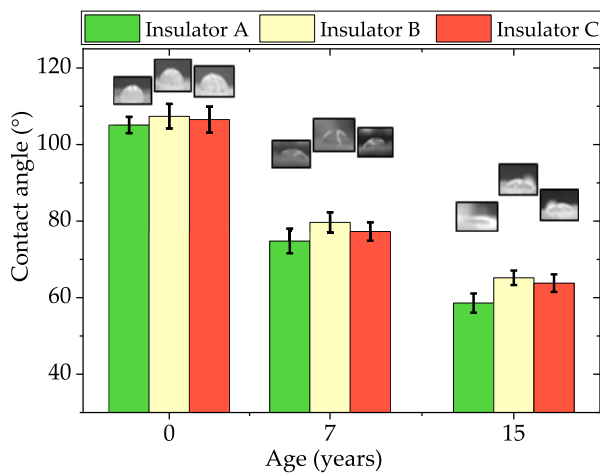


FIGURE 7. Contact angles of new and aged polymer insulators.

as follows:

$$e = \sum_{i=0}^m [lnI_i - (ln\alpha + \beta \cdot lnESDD_i + \gamma \cdot lnY_i)]^2 \quad (13)$$

where i is the data serial $i = (0, 1, 2, \dots, m)$. The coefficients α , β and γ in Equation (13) are extracted by calculating the minimum value of e , and the results of α , β , γ and R^2 are shown in Table 6.

According to fitting results in Figure 8 and Table 6, the correlation coefficients R^2 for all surfaces fitting are greater than 0.95, indicating the LC, ESDD and age of all insulators A, B and C fit of equations (11) under different levels of applied voltage and hydrophobic. It can be seen that the LC has the positive power function with ESDD and age of insulators, which means with an increase in both or either of ESDD and age the LC will increase.

The α values are affected by the structure and materials characteristics of the insulator, and the lower the value of the constant α is, the better the withstand LC. Due to the different structures of the selected insulator, different structure designs, and different creeping distances, the LC levels at the same conditions are different.

It can be observed from Table 6 that the values of the coefficient α of A, B and C insulator are different, and the α value of C insulator is lower than in the B and A,

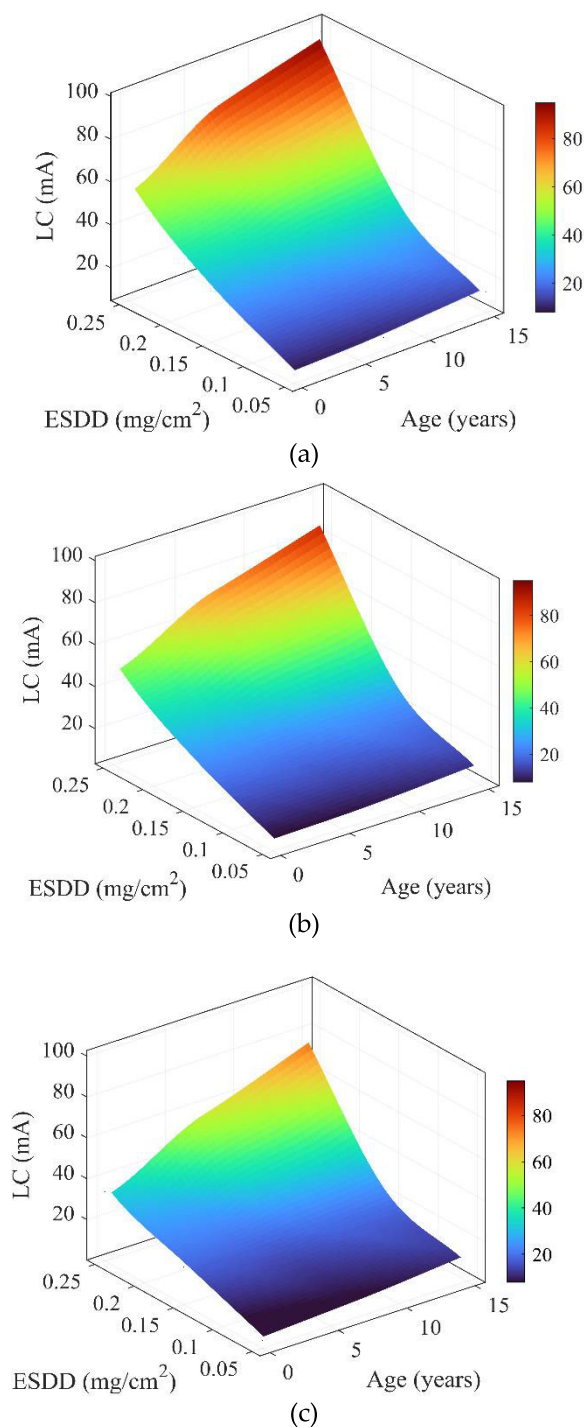


FIGURE 8. Fitting surface of the relationship between LC, ESDD, and age under applied voltage of 35 kV and HC3: (a) insulator A; (b) insulator B; (c) insulator C.

which means that C insulator has better performance. This is in line with the test findings in Tables 3 to 5, where insulator C exhibits the lowest LC compared to insulators A and B under identical conditions. β is the insulator’s characteristic pollution index. The bigger the β value indicates the greater the effect of pollution on the insulator LC value. The value

of β of insulator A the largest compared to its value with insulators B and C, which indicates that the insulator A is more influenced by pollution than the insulators B and C.

The value of γ is affected by the insulators ageing. The lower the value of γ is, the lower the LC is influenced by age of insulators. Also, the values of the coefficient γ are the lowest with insulator C compared to insulator A and B under same state. Exactly as stated in the previous subsection, the LC is the lowest with insulator C.

2) IMPACT OF APPLIED VOLTAGE ON LC AMPLITUDE

It is also important to study the influence of source strength on LC of new and aged insulators for various pollution and hydrophobicity levels. The LC results under different applied voltages are shown in Tables 3 to 5.

The results of tests depicted indicate that as U increases, the amplitude of LC for all insulators exhibits a rising trend. Taking the insulator type A under 0.15 mg/cm² and HC3 as an example, with the increase of U from 25 to 35 kV, LC increases from 6.62 mA to 30.76 mA when insulator is new, increasing by 365%; LC increases from 9.26 mA to 39.57 mA when insulator age is 7 years, increasing by 327%; LC increases from 10.7 mA to 49.97 mA when insulator age is 15 years, increasing by 367%. To demonstrate the influence of applied voltage on the LC of new and aged insulators, the surface fitting of the relationship between LC, U, and insulator age was displayed. Figure 9 shows the fitting surfaces of LC, U, and insulator age of insulators under 0.25 mg/cm² and HC3, which were performed using Equation (14) and the technique described in subsection III-C1

$$I = \alpha \cdot U^\beta \cdot Y^\gamma \tag{14}$$

Table 6 contains the values of α , β , γ , and R2 obtained through fitting the relationship between LC, U, and insulator age under specified levels of pollution and Hydrophobicity. Table 7 further shows that the difference between the numerical findings based on Equation (14) and the actual test results is minor, with R2 values greater than 0.95.

3) IMPACT OF INSULATOR HYDROPHOBICITY ON LC AMPLITUDE

To investigate the influence of hydrophobicity level on the LC performance of new and aged tested insulators, the relationship between hydrophobicity level and LC was proposed as in Equation (15):

$$I = \alpha \cdot HC^\beta \cdot Y^\gamma \tag{15}$$

The values of α , β , γ , and R2 were found using curve fitting showed in Figure 10 by least square error, and these coefficients have been given in Table 8.

As can be seen in Figure 9, LC increases exponentially with HC. This is due to the pollution layer on the insulator surface being more easily moistened, resulting in a reduction in surface resistance. It is worth mentioning that the value of β in Equation (15) represents the characteristic indicator of HC

TABLE 6. Leakage current test results in (mA) of ageing insulators of 15 years. ESDD in (mg/cm²) and U in (kV).

Insulator type		A			B			C		
HC	ESDD	0.05	0.15	0.25	0.05	0.15	0.25	0.05	0.15	0.25
	U									
1	25	4.26	9.84	25.87	3.20	11.48	21.18	2.55	10.73	19.73
	30	7.83	22.31	51.96	6.31	20.39	45.28	5.08	16.31	32.90
	35	13.26	31.89	57.53	9.76	27.91	50.08	8.72	23.16	42.20
3	25	5.23	10.70	31.90	4.00	14.26	26.37	3.18	13.37	24.52
	30	9.93	27.68	72.07	7.88	25.32	56.38	6.35	20.33	40.90
	35	22.85	49.97	75.60	17.20	44.66	70.25	15.90	42.85	65.32
5	25	7.01	21.17	42.74	5.66	19.10	37.44	4.52	18.99	34.67
	30	12.71	39.14	87.13	11.22	35.80	77.75	9.02	29.47	53.57
	35	25.44	57.38	125.2	17.32	50.26	114.3	15.26	40.80	103.6

on the insulator surface. According to Table 8, for specific values of U and ESDD, both α and β of insulator C have a minimal value when compared to their values in insulators A and B at all ages levels. This suggests that the influence of HC is minor in insulator C. This means that the insulator’s structure influences its performance. The next section will go through the relation between insulator structure and LC in depth.

4) IMPACT OF INSULATOR SHAPE ON LC AMPLITUDE

To study the effect shape of insulators on LC value, leakage distance L, equivalent diameter D_{eq} and form factor F were taken to consideration. According to the experimental results and Equations (16), the LC is influenced by the geometrical characteristics parameters L, D_{eq} and F. Under the ESDD of 0.15 mg/cm², HC = 3, U = 30 kV and different age, the impacts of L on LC of the insulators are illustrated in Figure 11(a), and the effect of D_{eq} on LC illustrated in Figure 11(b), as well as the effect F is illustrated in Figure 11(c).

The relations between leakage current and insulator’s geometrical parameters L, Deq and F are expressed as:

$$\left. \begin{aligned} I &= 226.8L^{-0.63} \cdot Y^{0.278}, & R^2 &= 0.978 \\ I &= 55.46D_{eq}^{-0.82} \cdot Y^{0.288}, & R^2 &= 0.964 \\ I &= 4.903e+06F^{-7.7} \cdot Y^{0.285}, & R^2 &= 0.957 \end{aligned} \right\} \quad (16)$$

With an increase in the leakage distance L, LC will decrease. LC will also decrease with the increase of the equivalent diameter or the increase of the form factor. L, D_{eq} , and F, on the other hand, have a close relationship. In order to reduce the LC of polluted insulators, the geometry of an insulator should be considered synthetically. Since the change in the value of γ is slight, it is possible to assume that the influence of insulator age on LC is almost the same whether correlated with L, D_{eq} , and F.

D. FLASHOVER VOLTAGE TEST RESULTS

Flashover is the minimum voltage required for an insulator to break down and allow current flow. As an insulator age,

its flashover voltage decreases, making it more likely to fail and become a safety hazard. Monitoring flashover voltage can therefore be used as a good indicator for insulator ageing. The polymeric insulators’ flashover voltage tests with AC voltage were carried out according to the procedure mentioned in section II-C. The results are displayed in Figure 12. Figure 12 shows, for unaged and aged insulators, the flashover voltage under a pollution effect based on the box chart and median values.

According to the chart, it is noticed that the flashover voltage decreased notably as insulators became older. Taking the insulator type A as an example, when the insulator’s time work is increased by seven years, the median values of flashover voltage decrease from 43.5 kV to 34.65 kV, a reduction of 20.34%, whereas for insulators that worked for 15 years, the median values of flashover voltage decrease from 43.5 kV to 22.5 kV, a reduction of 48.27%. The flashover voltage with the same insulator’s age in insulator C is significantly larger than in insulators A and B. For example, in insulator A, insulator B and insulator C, with the insulator’s age of 15 years, the median values of flashover voltage are 22.5 kV, 27.5 kV and 39 kV, respectively.

The relationship between flashover voltage and pollution severity in terms of ESDD in each bar are shown in Figure 12(b). There is a strong relationship between flashover voltage and pollution severity, as measured by ESDD. As ESDD increases, the flashover voltage of an insulator decreases. This is because pollution on the insulator’s surface decreases its effective resistance, allowing more current to flow and reducing the insulator’s overall dielectric strength.

IV. MODEL MODIFICATION

Figure 13 shows the equivalent circuit model of a polluted polymer insulator. The topology of the proposed model introduces the presence of pollution on the insulator surface and how pollution severity and insulator ageing can be managed using the model elements’ values. The proposed

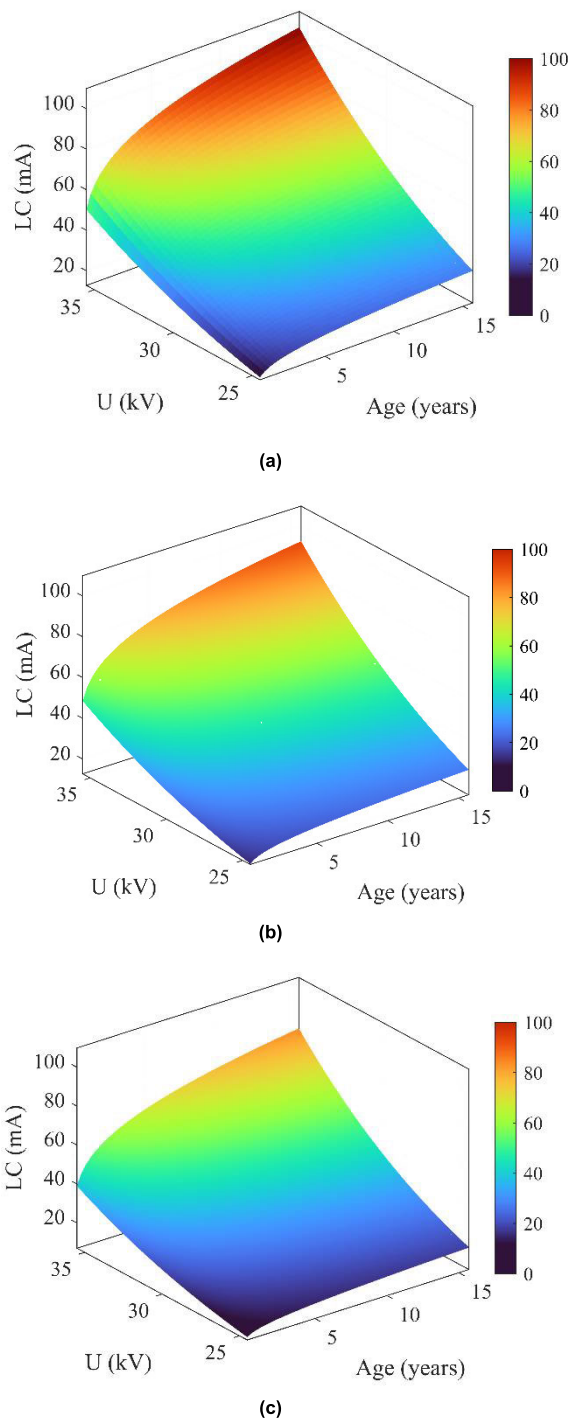


FIGURE 9. Fitting surface of the relationship between LC, U, and age under ESDD of 0.25 mg/cm² and HC3: (a) insulator A; (b) insulator B; (c) insulator C.

model is built from resistors and capacitors. The model is divided into three parts: the insulator part, the dry band part, and the pollution layer part. The initial parameters of the insulator that represented by resistance (R_s) in parallel with capacitance (C_s). The value of current passed through

TABLE 7. Fitting surface parameters of relationship between LC, ESDD.

Insulator						
	HC	U	α	β	γ	R2
A	1	25	97.62	1.423	0.211	0.959
		30	204.1	1.488	0.239	0.976
		35	267.8	1.517	0.261	0.997
	3	25	106.7	1.446	0.232	0.963
		30	213.8	1.512	0.320	0.993
		35	371.4	1.559	0.343	0.989
	5	25	109.2	1.494	0.372	0.984
		30	250.6	1.608	0.421	0.991
		35	400.3	1.613	0.442	0.992
B	1	25	74.93	1.350	0.203	0.981
		30	180.3	1.402	0.211	0.987
		35	234.8	1.419	0.242	0.985
	3	25	68.83	1.353	0.242	0.980
		30	125.3	1.505	0.311	0.986
		35	343.6	1.522	0.322	0.980
	5	25	109.1	1.331	0.369	0.988
		30	249.1	1.551	0.375	0.981
		35	354.2	1.532	0.401	0.983
C	1	25	58.1	1.321	0.147	0.989
		30	92.35	1.398	0.206	0.990
		35	218.4	1.224	0.224	0.971
	3	25	67.06	1.323	0.217	0.986
		30	113.9	1.393	0.302	0.992
		35	239.7	1.513	0.246	0.972
	5	25	85.86	1.325	0.345	0.985
		30	120.9	1.444	0.339	0.993
		35	329.2	1.508	0.383	0.978

elements R_s and C_s is used to calculate the insulator’s age. Meanwhile, the resistance (R_d) represents the dry band in the contamination film. The resistance R_p , which is located in series with the dry band, represents the wetted contamination layer. In the establishment of a contamination coat on the insulator surface, a parallel channel for LC, alongside the insulator material track, forms. Because of ohmic loss, LC produces heat as it flows. This heat generation is greater in areas with higher concentrations of LC, such as the insulator sleeve. Therefore, the contamination layer becomes dry in these regions, and dry bands format. It is worth mentioning that the dry band is a non-conductive film located between two conducting contamination layers, resulting in a capacitive impact.

Based on Obenaus’ suggested polluted insulator model [4] in Figure 13, the voltage across the pollution layer and dry band in the presence of an arc can be expressed as:

$$U_s = kxI^{-n} + R(x)I \tag{17}$$

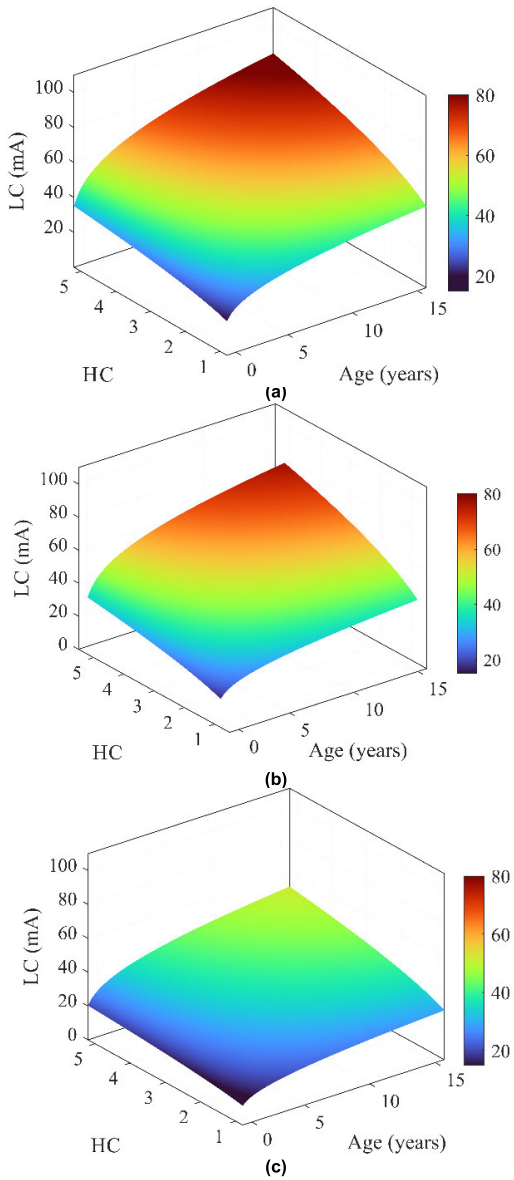


FIGURE 10. Fitting surface of the relationship between LC, U, and age under ESDD of 0.25 mg/cm² and HC3: (a) insulator A; (b) insulator B; (c) insulator C.

where I is the leakage current, $R(x)$ denotes the resistance of the contamination layer, x is the length of the arc and k and n represent the characteristic constants of the static arc that are obtained from laboratory tests. Deriving the voltage with respect to the current and setting the derived Equation to zero yields the current's critical value as in the following Equation.

$$\frac{dU_s}{dI} = -kxnI^{-n-1} + R(x) = 0 \tag{18}$$

From (14), the critical current is given by,

$$I_c = \left(\frac{kxn}{R(x)} \right)^{1/n+1} \tag{19}$$

TABLE 8. Fitting surface parameters of relationship between LC, U and insulator age.

Insulator						
	HC	ESDD	α	β	γ	R2
A	1	0.05	1.06×10^{-5}	3.27	0.144	0.961
		0.15	11.2×10^{-5}	3.41	0.167	0.962
		0.25	24.2×10^{-5}	3.43	0.179	0.981
	3	0.05	6.7×10^{-5}	3.45	0.215	0.955
		0.15	15.7×10^{-5}	4.32	0.221	0.997
		0.25	29.8×10^{-5}	4.43	0.279	0.982
	5	0.05	11.4×10^{-5}	3.67	0.216	0.952
		0.15	38.3×10^{-5}	3.81	0.344	0.962
		0.25	43.1×10^{-5}	5.13	0.362	0.974
B	1	0.05	1.44×10^{-5}	2.57	0.126	0.964
		0.15	4.82×10^{-5}	3.12	0.138	0.986
		0.25	18.3×10^{-5}	3.45	0.155	0.964
	3	0.05	5.5×10^{-5}	2.67	0.161	0.986
		0.15	12.4×10^{-5}	3.33	0.183	0.973
		0.25	23.1×10^{-5}	3.67	0.221	0.991
	5	0.05	27.4×10^{-5}	3.52	0.196	0.982
		0.15	33.3×10^{-5}	3.72	0.282	0.965
		0.25	39.8×10^{-5}	3.88	0.282	0.977
C	1	0.05	1.12×10^{-5}	2.44	0.121	0.963
		0.15	3.98×10^{-5}	3.10	0.128	0.977
		0.25	16.7×10^{-5}	3.21	0.146	0.974
	3	0.05	4.4×10^{-5}	2.58	0.156	0.962
		0.15	9.6×10^{-5}	3.17	0.177	0.958
		0.25	20.9×10^{-5}	3.48	0.205	0.982
	5	0.05	25.8×10^{-5}	3.39	0.183	0.971
		0.15	26.5×10^{-5}	3.61	0.269	0.965
		0.25	28.7×10^{-5}	3.75	0.277	0.992

The surface resistance $R(x)$ was described as the division of the shape coefficient of sample (f) and the pollution layer conductivity (σ):

$$R(x) = \frac{f}{\sigma} \tag{20}$$

where σ is the pollution layer electrical conductivity. As stated in [4], the conductivity of the surface pollution layer can be expressed in relation to ESDD as

$$\sigma = 86.ESDD^{0.9} \tag{21}$$

The shape coefficient f is calculated as in [29]

$$f = \int_0^L \frac{dx}{\pi D(x)} = \frac{L}{D_{eq}} \tag{22}$$

where L is leakage distance of insulator, $D(x)$ is the diameter of insulator, where the length is x . D_{eq} is the equivalent

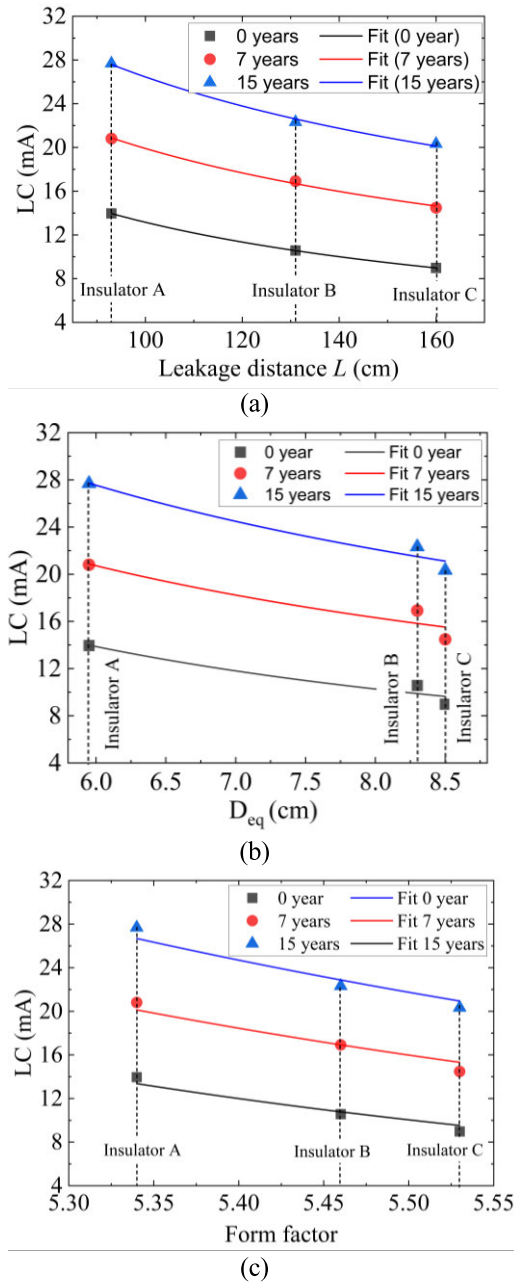


FIGURE 11. The relationship between LC and insulators geometrical parameters under ESDD of 0.15 mg/cm^2 , U of 30 kV and different age: (a) Leakage distance L ; (b) Equivalent diameter D_{eq} ; (c) Form Factor F .

diameter of insulator. To approximate the equivalent diameter of long rod insulators, the average diameter of the trunks and the sheds can be calculated using the following Equation,

$$D_{eq} = \frac{\sum_{j=1}^{N_{tr}} D_j}{N_{tr}} + \frac{\sum_{k=1}^{N_{shb}} D_k}{N_{shb}} + \frac{\sum_{m=1}^{N_{shs}} D_m}{N_{shs}} \quad (23)$$

where D_j , D_k , D_m represent the diameter of each trunk, the diameter of each big shed and the diameter of each

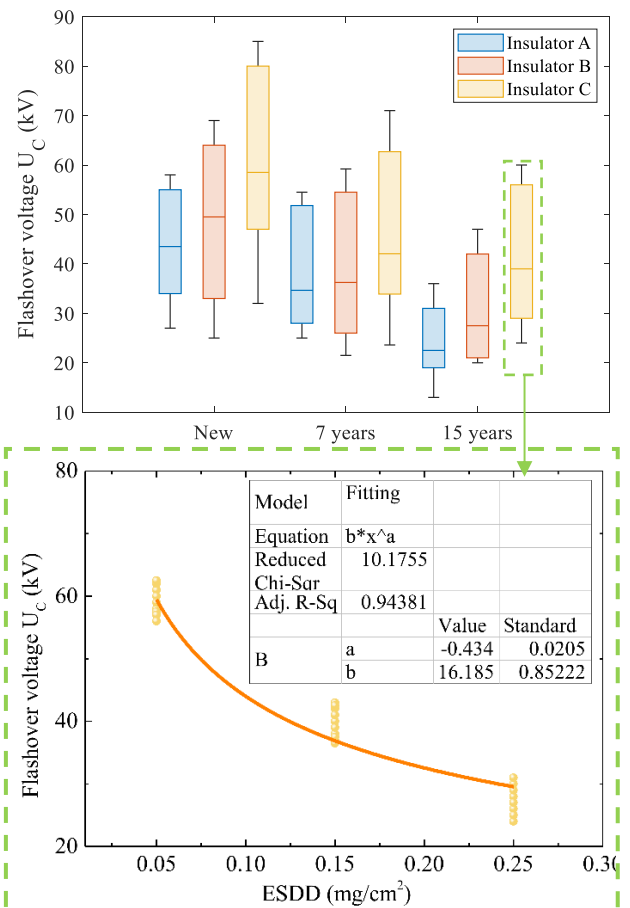


FIGURE 12. Flashover voltage via insulator ageing (a), under different pollution severity (b).

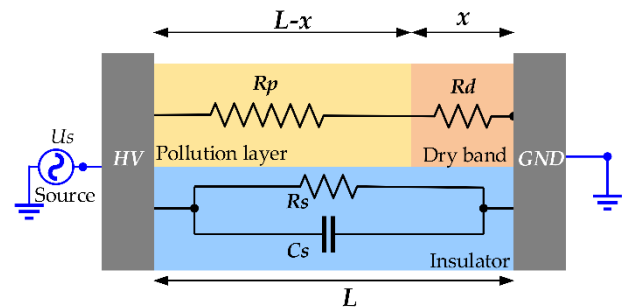


FIGURE 13. Equivalent circuit of polluted insulator.

small shed, respectively. N_{tr} , N_{shb} , N_{shs} represent the number of trunk, big sheds and small sheds, respectively.

Then, the Equation (20) can be rewritten as

$$R(x) = \frac{L}{\sigma D_{eq}} \quad (24)$$

Substituting (24) into (19) yields:

$$I_c = \left(\frac{kx n \sigma D_{eq}}{L} \right)^{1/n+1} \quad (25)$$

Substituting (21) into (25) yields:

$$I_c = \left(\frac{kx n D_{eq} (86ESDD^{0.9})}{L} \right)^{1/n+1} \quad (26)$$

The critical LC of insulators as a function of ESDD or any insulator's geometrical characteristic can be estimated using the proposed LC model in Equation (26). The critical flashover voltage U_c is predicted as:

$$U_c = k \frac{1}{n+1} r_p^{\frac{n}{n+1}} L \quad (27)$$

Taking into account the accumulation of current at the arc root point, the rp can be written as [37]:

$$r_p = \frac{f}{L\sigma} \ln \frac{L-x}{r_0}, \quad r_0 = \sqrt{\frac{I_c}{1.45\pi}} \quad (28)$$

where r_0 is arc root radius. According to Equations (26), (27) and (28), the critical flashover voltage U_c can be expressed as:

$$U_c = k \frac{1}{n+1} \left(\frac{f}{L\sigma} \ln \frac{L-x}{\sqrt{\left(\frac{kx n D_{eq} (86ESDD^{0.9})}{L} \right)^{1/n+1} / 1.45\pi}} \right)^{\frac{n}{n+1}} L \quad (29)$$

The critical flashover voltage model results are presented in comparison with the experimental data and ANN model results in section VI.

To compute the effect of insulator age on LC based proposed model, the arc characteristic k and n were determined using adopting regression analysis of $E_{arc}-I_{arc}$ characteristic as in Equation (30).

$$E_{arc} = k I_{arc}^{-n} \quad (30)$$

where E is the arc voltage gradient. Many tests were carried out to produce the static $E_{arc}-I_{arc}$ characteristic of aged and aged insulators at 15 cm of arc length, and the results of tests are shown in Figure 14. The values of k and n were extracted from the fitting the relationship between E_{arc} and I_{arc} , the k and n findings are presented in Table 9.

A. EQUATIONS

To validate the model of the critical LC of insulators, it was used to all insulators aged 7 and 15 years. The results were then compared to the experimental ones. Based on the characteristics of arc in Table 9, the critical LC model in Equation (26) was calculated for three insulators. The results of the model were compared with experimental results and ANN model and shown in section VI.

V. ANN MODEL

ANN is a predictive modeling approach used in industrial applications to replace high computational cost experiments by generating a model containing trial parameters and responses. ANN models are helpful when empirical equations cannot identify process parameters. ANNs have

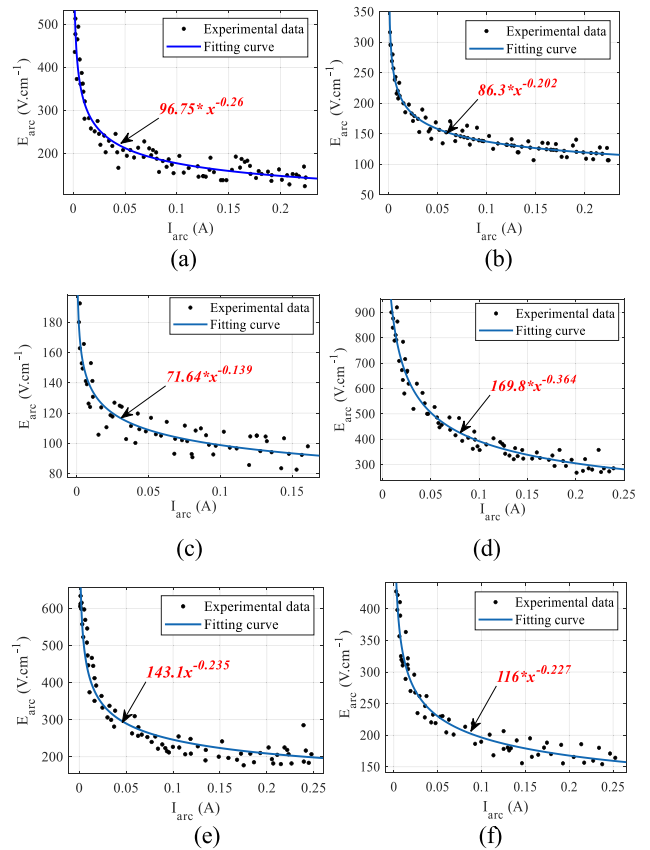


FIGURE 14. Static Earc-Iarc characteristic of the AC arc under ESDD=0.35mg/cm², U=35 kV and HC = 3 at different insulator age:(a), (b), (c) 7 years; (d), (e), (f) 15 years.

input, hidden, and output layers. Neurons expressing these variables make up the input and output layers. One or two concealed layers are ideal. Single output ANN models perform better [38]. Each layer contains fixed neurons with configurable weights. The inaccuracy is lessened by adjusting these weights throughout training. In this paper, the ANN's accurate predictions were made using a widely used multilayer backpropagation neural network with the Levenberge Marquardt [39] learning algorithm using MATLAB (R2021a) software. According to [40], the reason for employing the second order nonlinear Levenberg Marquardt algorithm is its quicker operation by auto error correction in the learning parameters. By ensuring a curvilinear fit between the inputs and outputs of the cells, the right activation function would greatly improve the network performance. The logistic sigmoid (log sig) transfer function was extensively employed as an activation function in this work. Before training, the neural input and output data were standardized using Equation (31) between $\lambda_1 = 0.1$ and $\lambda_2 = 0.9$ [41].

$$Z_i = \lambda_1 + (\lambda_2 - \lambda_1) \left(\frac{\chi_i - \chi_{i,\min}}{\chi_{i,\max} - \chi_{i,\min}} \right) = 0.1 + 0.8 \times \left(\frac{\chi_i - \chi_{i,\min}}{\chi_{i,\max} - \chi_{i,\min}} \right) \quad (31)$$

TABLE 9. Fitting surface parameters of relationship between LC, HC and insulator age.

Insulator	HC	ESDD	α	β	γ	R2	
A	1	0.05	1.36	0.19	0.238	0.978	
		0.15	3.68	0.21	0.304	0.947	
		0.25	11.73	0.24	0.319	0.979	
	3	0.05	3.77	0.23	0.243	0.956	
		0.15	14.84	0.24	0.282	0.971	
		0.25	27.28	0.27	0.313	0.967	
	5	0.05	8.37	0.24	0.243	0.964	
		0.15	22.52	0.25	0.291	0.952	
		0.25	34.89	0.28	0.318	0.963	
	B	1	0.05	1.23	0.17	0.235	0.962
			0.15	2.81	0.19	0.303	0.951
			0.25	8.84	0.22	0.316	0.977
3		0.05	3.33	0.2	0.208	0.963	
		0.15	12.32	0.23	0.266	0.977	
		0.25	23.9	0.206	0.311	0.953	
5		0.05	5.23	0.22	0.272	0.965	
		0.15	18.91	0.22	0.280	0.959	
		0.25	26.59	0.26	0.316	0.949	
C		1	0.05	0.983	0.14	0.172	0.982
			0.15	1.73	0.16	0.213	0.979
			0.25	3.56	0.19	0.301	0.961
	3	0.05	1.82	0.15	0.196	0.973	
		0.15	7.32	0.16	0.232	0.966	
		0.25	16.22	0.203	0.308	0.961	
	5	0.05	4.28	0.17	0.243	0.948	
		0.15	10.37	0.19	0.261	0.984	
		0.25	18.89	0.23	0.313	0.991	

Zi represent the standardized value of χ_i , and $\chi_{i,\min}$ and $\chi_{i,\max}$ are the minimum and maximum of χ_i , respectively. The ANN structure is demonstrated in Figure 15. ESDD, f, Deq, age, U and HC are six different inputs, and the LC or flashover voltage U_c is the output obtained from the ANN model. A total of 242 data points is utilized as inputs for the ANN model, 170 (70%) of which were used for training, 36 (15%) for validation, and 36 (15%) for testing. The hidden neurons number of ANN model topology was selected according to the micro ribonucleic acid recognition element (MRE) value. The number of layers that yielded the minimum MRE value was set for training the model, so the ANN model topology is 6-10-1 (Figure 15).

The ANN training was carried out across 50 epochs, where found the optimal results at this point. The Artificial Neural Network (ANN) had an automated process for determining each neuron's starting weights and biases

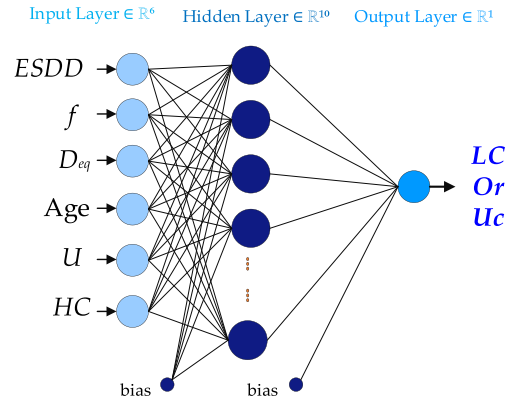


FIGURE 15. ANN model.

when training began. Training of the network ceased either when the minimum mean squared error (MSE) was achieved at the maximum epoch or when the minimum gradient reached a specified benchmark level. The minimum gradient was 10^{-7} , and the maximum number of iterations was 1000.

VI. COMPARISON OF THE ANN MODEL AND MODIFIED MODEL

Figure 16 compares the LC and critical flashover voltage U_c findings obtained from experiments with the proposed models' results. It can be observed that the computed results of the LC models are in good agreement with the test results. The deviation error was found to be below 10.2%, 4.67% and 8.27%, respectively, for the modified model, ANN and Equation (11) (Fitting Equation) in all cases. This indicates that the developed models are adequate in relating the main factors with the responses and efficiently predict the LC of insulators under different conditions without performing actual experiments, as shown in Figure 16. Moreover, the results revealed that the ANN model performs better compared to other models for making LC of polluted insulators predictions. The equations presented below can be used to assess the statistical performance of the suggested models, including ANN and mathematical models, based on measures such as RMSE, MSE, R2, and AAD.

$$RMSE = \left(\frac{1}{n} \sum_{i=1}^n (v_{i,m} - v_{i,e})^2 \right)^{0.5} \quad (32)$$

$$MSE = \frac{1}{n} \sum_{i=1}^n (v_{i,m} - v_{i,e})^2 \quad (33)$$

$$R^2 = 1 - \left(\frac{\sum_{i=1}^n (v_{i,m} - v_{i,e})^2}{\sum_{i=1}^n (v_{i,e} - v_{av})^2} \right) \quad (34)$$

$$AAD = \left(\frac{1}{n} \sum_{i=1}^n \left(\frac{(v_{i,m} - v_{i,e})}{(v_{i,e})} \right) \right) \times 100\% \quad (35)$$

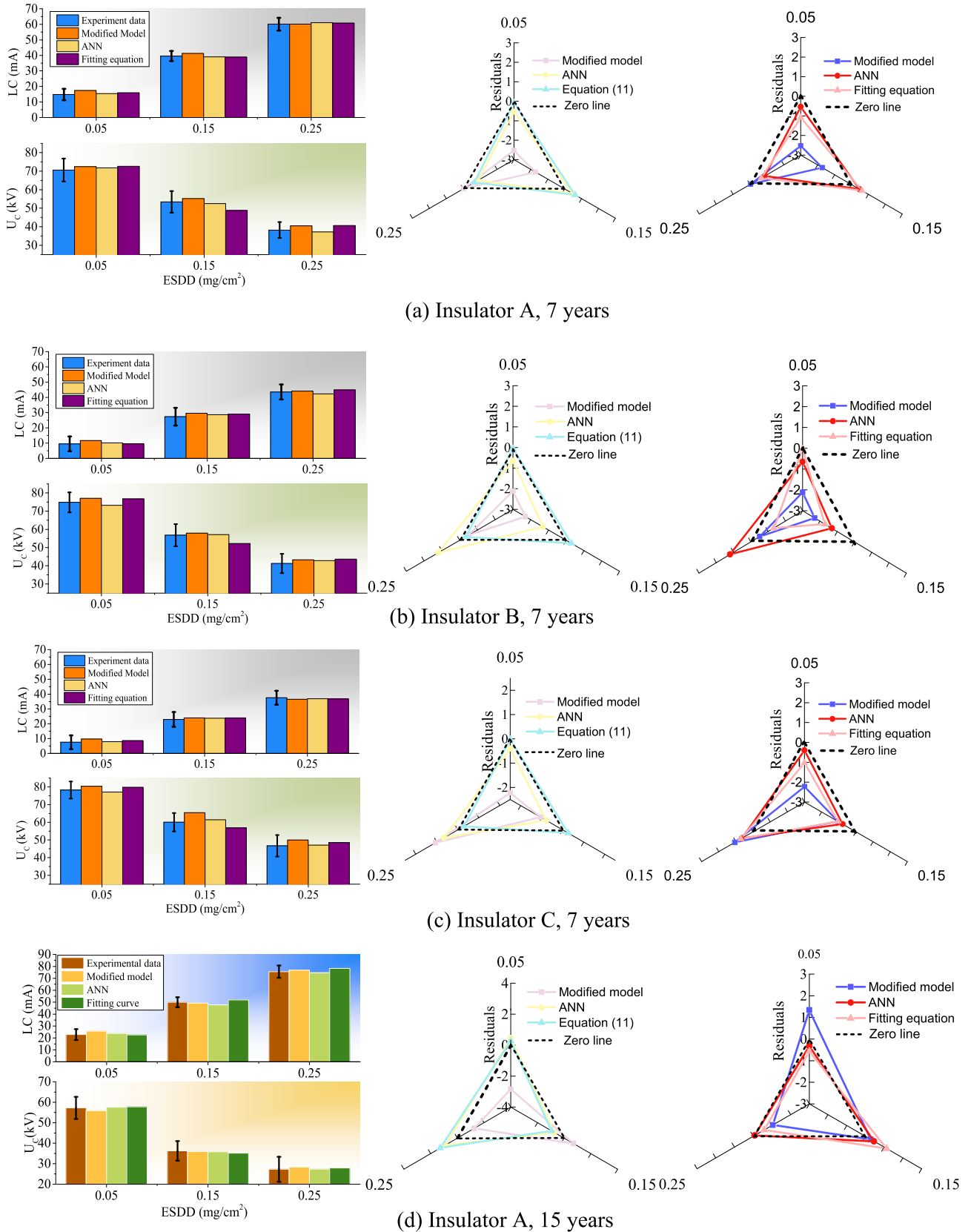


FIGURE 16. Comparison of calculated LC and U_c models and tested results under $U=35$ kV and $HC = 3$ at different insulator age:(a), (b), (c) 7 years; (d), (e), (f) 15 years.

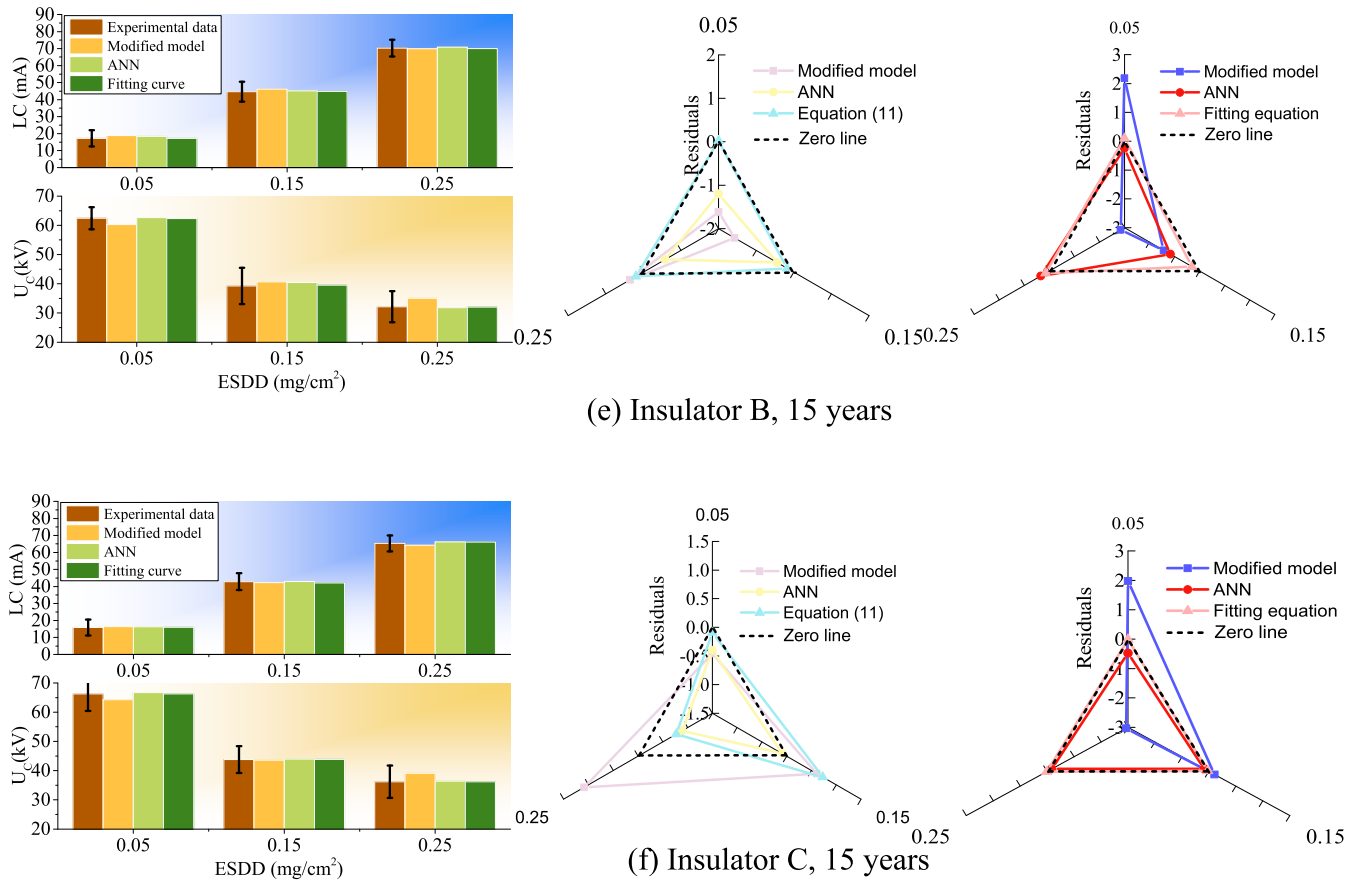


FIGURE 16. (Continued.) Comparison of calculated LC and U_c models and tested results under $U=35$ kV and $HC = 3$ at different insulator age:(a), (b), (c) 7 years; (d), (e), (f) 15 years.

TABLE 10. Arc constant k and n under ESDD=0.35mg/cm.

Insulator type		7 years	15 years
A	k	96.75	196.8
	n	0.26	0.364
	R2	0.987	0.991
B	k	86.3	143.1
	n	0.202	0.235
	R2	0.992	0.982
C	k	71.64	116
	n	0.139	0.227
	R2	0.974	0.983

where n represents the points number, $v_{i,e}$ is the experimental value at i point, $v_{i,m}$ is the model value at i point and v_{av} is the average of experimental values.

Table 9 depicts the statistical errors calculated to compare the predicted results from the presented models. Consider an insulator with seven years as an example; it is worth noting that the R2 values of predicted LC at insulator A, insulator B,

and insulator C results for the modified model were 0.973, 0.988 and 0.983, respectively. In the case of the ANN model, the R^2 values were 0.997, 0.995 and 0.996 for insulator A, insulator B, and insulator C, respectively. While in the case of the fitting model by Equation (11), the R^2 values were 0.994, 0.990 and 0.985 for insulator A, insulator B, and insulator C, respectively. Also, the R^2 values of predicted critical flashover voltage U_c were the largest with ANN model. The findings in Table 10 indicate that the ANN model is superior to other models for predicting the LC values for all cases. Furthermore, ANN can predict any data in nonlinearity behavior; it can readily defeat the restriction of the fitting model, such as a rapid shift of data trend if the insulator condition changes. The Fitting technique, in contrast to the ANN model, has the advantage of offering regression equations for prediction in addition to showing and classifying insignificant key variables, interaction factors, or insignificant quadratic terms in the approach, and as a result, can reduce the problem's sophistication.

While the mathematical model can be used to characterize and generate new parameters for practical models, it can also be used to predict the required parameter, as observed by another previous studies [42], [43].

TABLE 11. Statistical indicators comparison between modified model, ANN and fitting model.

Insulator		A			B			C			
	Age	Modified	ANN	Fit	Modified	ANN	Fit	Modified	ANN	Fit	
Ic	RMSE	7	1.762	0.655	0.824	1.830	1.092	1.185	1.547	0.630	0.938
		15	1.839	0.718	0.934	1.318	0.810	0.825	0.766	0.566	0.614
	MSE	7	3.127	0.429	0.673	3.353	1.193	1.405	2.394	0.397	0.881
		15	3.384	0.515	0.873	1.738	0.657	0.680	0.587	0.320	0.377
	R2	7	0.973	0.997	0.994	0.988	0.995	0.990	0.983	0.996	0.985
		15	0.982	0.998	0.993	0.979	0.999	0.992	0.971	0.997	0.991
ADD	7	1.030	0.056	0.189	1.882	0.256	0.163	3.025	0.143	0.707	
	15	0.532	0.025	0.026	0.336	0.168	0.542	0.044	0.027	0.015	
Uc	RMSE	7	2.213	0.734	1.023	1.973	0.882	0.821	1.693	0.789	1.062
		15	3.037	0.993	1.315	1.845	0.832	0.981	1.755	1.123	1.122
	MSE	7	3.414	0.576	1.885	2.658	2.234	1.038	2.144	0.959	0.831
		15	3.618	0.923	0.654	1.111	1.932	1.176	1.398	1.265	0.993
	R2	7	0.963	0.993	0.944	0.967	0.999	0.948	0.973	0.993	0.969
		15	0.972	0.991	0.996	0.962	0.998	0.991	0.975	0.996	0.992
ADD	7	1.112	0.055	0.167	2.224	0.448	0.132	2.341	0.233	0.948	
	15	0.834	0.063	0.034	0.534	0.324	0.667	1.562	0.693	1.423	

VII. CONCLUSION

The work carried out in this research paper has investigated the effect of pollution severity, ageing, geometrical structure, and hydrophobicity class on polymeric insulators' LC amplitudes. This comprehensive study investigates the LC value, enabling the assessment and prediction of the status of aged insulators in transmission and distribution lines subjected to varying wet, pollution, and changes in source voltage. The study's conclusions are drawn into the following points.

- Insulator LC is affected not only by the degree of contamination, but also by the insulators' age, HC, and geometrical characteristics.

- The LC increases exponentially with the age of the insulator; with the same age, the LC value is high in insulators with low values of leakage distance, equivalent diameter, and form factor.

- The equations of the relationship between LC, ESDD, and insulator age for all insulators, the relationship between LC, U , and insulator age, and the relationship between LC, HC, and insulator age are established and validated. The relative errors between the calculated and test values are within acceptable ranges, less than 10%, indicating that the equations are accurate.

- The critical flashover voltage was measured and computed for unaged and aged insulators. The results showed that the critical flashover voltage decreases as the age of insulators increases.

- Three models, namely the fitting model, mathematic model and ANN model were proposed to predict LC and U_c of insulators under different conditions, and the prediction results are consistent with the actual measured critical LC and U_c with deviations less than 10.5% for all cases.

- Statistical analyses of the models' performance indicated that the ANN model performs better than the other models. However, the mathematical model must be used because it indicates the influence of each ingredient and the direction of its effect, either negatively or positively.

- Computing the current of contaminated insulators using the proposed model has shown promising results in predicting the condition of aged insulators. In addition, it can be successfully used with any type of insulator under varying conditions to make accurate predictions about the insulators' states.

REFERENCES

- [1] M. Taghvaei, M. Sedighzadeh, N. NayebPashae, and A. S. Fini, "Reliability assessment of RTV and nano-RTV-coated insulators concerning contamination severity," *Electr. Power Syst. Res.*, vol. 191, Feb. 2021, Art. no. 106892.
- [2] D. Pinzan, F. Branco, M. A. Haddad, M. E. A. Slama, M. Albano, R. T. Waters, and H. Leite, "Performance of composite outdoor insulator under superimposed direct and switching impulse voltages," *IEEE Trans. Power Del.*, vol. 36, no. 2, pp. 1193–1201, Apr. 2021.
- [3] S. F. Stefenon, L. O. Seman, N. F. S. Neto, L. H. Meyer, A. Nied, and K.-C. Yow, "Echo state network applied for classification of medium voltage insulators," *Int. J. Electr. Power Energy Syst.*, vol. 134, Jan. 2022, Art. no. 107336.
- [4] A. A. Salem, R. A. Rahman, and S. Al-Ameri, "Pollution flashover characteristics of high-voltage outdoor insulators: Analytical study," *Arabian J. Sci. Eng.*, vol. 47, no. 3, pp. 2711–2729, Mar. 2022.
- [5] M. F. Palangar, U. Amin, H. Bakhshayesh, G. Ahmad, A. Abu-Siada, and M. Mirzaie, "Identification of composite insulator criticality based on a new leakage current diagnostic index," *IEEE Trans. Instrum. Meas.*, vol. 70, pp. 1–10, 2021.
- [6] R. Jayabal, V. Karuppiyan, and R. K. Sidharthan, "Naive Bayesian classifier for hydrophobicity classification of overhead polymeric insulators using binary image features with ambient light compensation," *High Voltage*, vol. 4, no. 4, pp. 324–332, Dec. 2019.
- [7] M. Z. Saleem and M. Akbar, "Review of the performance of high-voltage composite insulators," *Polymers*, vol. 14, no. 3, p. 431, Jan. 2022.

- [8] Y. Liu, X. Kong, Y. Wu, and B. Du, "Dynamic behavior of droplets and flashover characteristics for CFD and experimental analysis on SiR composites," *IEEE Access*, vol. 7, pp. 8095–8101, 2019.
- [9] Arshad, A. Nekahi, S. G. Mcmeekin, and M. Farzaneh, "Measurement of surface resistance of silicone rubber sheets under polluted and dry band conditions," *Electr. Eng.*, vol. 100, no. 3, pp. 1729–1738, Sep. 2018.
- [10] Y. Lin, F. Yin, Y. Liu, L. Wang, Y. Zhao, and M. Farzaneh, "Effect of ultraviolet—A radiation on surface structure, thermal, and mechanical and electrical properties of liquid silicone rubber," *J. Appl. Polym. Sci.*, vol. 136, no. 24, p. 47652, Jun. 2019.
- [11] D. Ghosh and D. Khastgir, "Degradation and stability of polymeric high-voltage insulators and prediction of their service life through environmental and accelerated aging processes," *ACS Omega*, vol. 3, no. 9, pp. 11317–11330, Sep. 2018.
- [12] M. E. A. Abed, H. Hadi, M. E. A. Slama, A. W. Belarbi, and N. Zekri, "Experimental investigation on dielectric/electric properties of aged polymeric insulator: Correlation of permittivity and dielectric loss tangent with surface hydrophobicity," *Electr. Eng.*, vol. 104, no. 3, pp. 1539–1552, Jun. 2022.
- [13] K. Sit, A. K. Pradhan, B. Chatterjee, and S. Dalai, "A review on characteristics and assessment techniques of high voltage silicone rubber insulator," *IEEE Trans. Dielectr. Electr. Insul.*, vol. 29, no. 5, pp. 1889–1903, Oct. 2022.
- [14] R. T. Waters, A. Haddad, H. Griffiths, N. Harid, P. Charalampidis, and P. Sarkar, "Dry-band discharges on polluted silicone rubber insulation: Control and characterization," *IEEE Trans. Dielectr. Electr. Insul.*, vol. 18, no. 6, pp. 1995–2003, Dec. 2011.
- [15] Z. Zhang, X. Liu, X. Jiang, J. Hu, and D. W. Gao, "Study on AC flashover performance for different types of porcelain and glass insulators with non-uniform pollution," *IEEE Trans. Power Del.*, vol. 28, no. 3, pp. 1691–1698, Jul. 2013.
- [16] J. D. Samakosh and M. Mirzaie, "Experimental-based models for predicting the flashover voltage of polluted SiR insulators using leakage current characteristics," *IET Sci., Meas. Technol.*, vol. 14, no. 10, pp. 943–952, Dec. 2020.
- [17] A. A. Salem, K. Y. Lau, Z. Abdul-Malek, N. Mohammed, A. M. Al-Shaalan, A. A. Al-Shamma'a, and H. M. H. Farh, "Polymeric insulator conditions estimation by using leakage current characteristics based on simulation and experimental investigation," *Polymers*, vol. 14, no. 4, p. 737, Feb. 2022.
- [18] J. D. Samakosh and M. Mirzaie, "Analysis of leakage current characteristics during aging process of SiR insulator under uniform and longitudinal non-uniform pollution conditions," *Measurement*, vol. 147, Dec. 2019, Art. no. 106862.
- [19] S. Mohammadnabi and K. Rahmani, "Influence of humidity and contamination on the leakage current of 230-kV composite insulator," *Electr. Power Syst. Res.*, vol. 194, May 2021, Art. no. 107083.
- [20] A. Rashid, M. Amin, M. Ali, and A. Khattak, "Aging exploration of long term multistressed HTV-silicone rubber/silica/alumina composites for high voltage insulation," *Mater. Res. Exp.*, vol. 5, no. 9, Aug. 2018, Art. no. 095301.
- [21] L. Cui and M. Ramesh, "Prediction of flashover voltage using electric field measurement on clean and polluted insulators," *Int. J. Electr. Power Energy Syst.*, vol. 116, Mar. 2020, Art. no. 105574.
- [22] H. Kordkheili, H. Abravesh, M. Tabasi, M. Dakhem, and M. Abravesh, "Determining the probability of flashover occurrence in composite insulators by using leakage current harmonic components," *IEEE Trans. Dielectr. Electr. Insul.*, vol. 17, no. 2, pp. 502–512, Apr. 2010.
- [23] X. Jiang, Y. Guo, Z. Meng, Z. Li, and Z. Jiang, "Additional salt deposit density of polluted insulators in salt fog," *IET Gener., Transmiss. Distrib.*, vol. 10, no. 15, pp. 3691–3697, Nov. 2016.
- [24] N. F. S. Neto, S. F. Stefenon, L. H. Meyer, R. G. Ovejero, and V. R. Q. Leithardt, "Fault prediction based on leakage current in contaminated insulators using enhanced time series forecasting models," *Sensors*, vol. 22, no. 16, p. 6121, Aug. 2022.
- [25] Y. Li, H. Yang, Q. Zhang, X. Yang, X. Yu, and J. Zhou, "Pollution flashover calculation model based on characteristics of AC partial arc on top and bottom wet-polluted dielectric surfaces," *IEEE Trans. Dielectr. Electr. Insul.*, vol. 21, no. 4, pp. 1735–1746, Aug. 2014.
- [26] X. Jiang, J. Yuan, L. Shu, Z. Zhang, J. Hu, and F. Mao, "Comparison of DC pollution flashover performances of various types of porcelain, glass, and composite insulators," *IEEE Trans. Power Del.*, vol. 23, no. 2, pp. 1183–1190, Apr. 2008.
- [27] M. Wang, Y. Yuan, X. Jiang, T. Li, Q. Chen, and F. Zhou, "Switching impulse flashover performance of nonuniform pollution insulators in natural environment," *IEEE Trans. Dielectr. Electr. Insul.*, vol. 30, no. 2, pp. 844–851, Apr. 2023.
- [28] A. A. Salem, R. A. Rahman, M. S. Kamarudin, N. A. Othman, N. A. M. Jamail, H. A. Hamid, and M. T. Ishak, "An alternative approaches to predict flashover voltage on polluted outdoor insulators using artificial intelligence techniques," *Bull. Electr. Eng. Informat.*, vol. 9, no. 2, pp. 533–541, Apr. 2020.
- [29] S. Yang, Z. Jia, and X. Ouyang, "Effects of asymmetrical algal distribution on the AC flashover characteristics of bio-contaminated silicone rubber insulators," *Electr. Power Syst. Res.*, vol. 172, pp. 296–302, Jul. 2019.
- [30] *Artificial Pollution Tests on High Voltage Insulators to be Used on AC Systems*, Standard IEC 60507, 3rd ed., IEC, 2013.
- [31] *Selection and Dimensioning of High-Voltage Insulators for Polluted Conditions—Part 1: Definitions, Information and General Principles*, Standard IEC 60815, International Electrotechnical Commission, Geneva, Switzerland, 2008.
- [32] A. A. Salem, K. Y. Lau, Z. Abdul-Malek, W. Zhou, S. Al-Ameri, S. A. Al-Gailani, and R. A. Rahman, "Investigation of high voltage polymeric insulators performance under wet pollution," *Polymers*, vol. 14, no. 6, p. 1236, Mar. 2022.
- [33] *STRI Guide 92/1 STRI GUIDE 92/1 Hydrophobicity Classification Guide*, Hydrophobicity classified Guide, 1992, p. 9.
- [34] A. A. Salem, K. Y. Lau, Z. Abdul-Malek, and C. W. Tan, "Classifying insulator conditions of room temperature vulcanized coated glass insulators under different coating damage modes," *Measurement*, vol. 194, May 2022, Art. no. 111032.
- [35] A. A. Salem, K. Y. Lau, W. Rahiman, S. A. Al-Gailani, Z. Abdul-Malek, R. Abd Rahman, S. M. Al-Ameri, and U. U. Sheikh, "Pollution flashover characteristics of coated insulators under different profiles of coating damage," *Coatings*, vol. 11, no. 10, p. 1194, Sep. 2021.
- [36] F. Obenaus, "Fremdschichtueberschlag und kriechwegeange," *Deutsche Elektrotechnik*, vol. 4, pp. 135–137, 1958.
- [37] T. Özel and Y. Karpat, "Predictive modeling of surface roughness and tool wear in hard turning using regression and neural networks," *Int. J. Mach. Tools Manuf.*, vol. 45, nos. 4–5, pp. 467–479, Apr. 2005.
- [38] O. E. Gouda and D. M. Khalifa, "Online monitoring of medium voltage overhead distribution lines polluted insulators severity," *CIREOpen Access Proc. J.*, vol. 2017, no. 1, pp. 372–375, Oct. 2017.
- [39] S. Kullolli, G. Sakthivel, and M. Ilankumaran, "A neural network model for the prediction of compression ignition engine performance at different injection timings," *Int. J. Ambient Energy*, vol. 37, no. 3, pp. 227–236, May 2016.
- [40] A. A. Salem, K. Y. Lau, Z. Abdul-Malek, S. A. Al-Gailani, and C. W. Tan, "Flashover voltage of porcelain insulator under various pollution distributions: Experiment and modeling," *Electr. Power Syst. Res.*, vol. 208, Jul. 2022, Art. no. 107867.
- [41] M. F. Palangar and M. Mirzaie, "Mathematical modeling of critical parameters on the polluted ceramic insulators under AC voltage: Based on experimental tests," *Arabian J. Sci. Eng.*, vol. 41, no. 9, pp. 3501–3510, Sep. 2016.
- [42] M. F. Palangar, M. Mirzaie, and A. Mahmoudi, "Improved flashover mathematical model of polluted insulators: A dynamic analysis of the electric arc parameters," *Electr. Power Syst. Res.*, vol. 179, Feb. 2020, Art. no. 106083.
- [43] A. Salem, R. Abd-Rahman, W. Ghanem, S. Al-Gailani, and S. Al-Ameri, "Prediction flashover voltage on polluted porcelain insulator using ANN," *Comput., Mater. Continua*, vol. 68, no. 3, pp. 3755–3771, 2021.



ALI AHMED SALEM (Member, IEEE) received the M.Eng. degree in electrical power engineering from University Tun Hussein Onn Malaysia (UTHM), in 2016, and the Ph.D. degree in high-voltage from the Faculty of Electrical Engineering, UTHM, in 2021. He has been a Post-Doctoral Fellow with Universiti Teknologi Malaysia (UTM) Grantee for 2 years. Currently, he is a Senior Lecturer with the School of Electrical Engineering, Universiti Teknologi MARA (UiTM), Shah Alam. His current research interest includes the dynamic arc modeling of pollution flashover on high voltage outdoor insulators.



AHMED ALLAWY ALAWADY received the B.Eng. degree in electrical engineering from the University of Kufa, Iraq, in 2007, and the M.Eng. degree in electrical power systems from SHUATS, India, in 2012. He is currently pursuing the Ph.D. degree with Universiti Tun Hussein Onn Malaysia (UTHM). He has been a Lecturer with the College of Technical Engineering, Islamic University, Iraq, since 2007. His current research interest includes motors fault detection using the frequency response analysis (FRA) technique.



KWAN YIEW LAU (Senior Member, IEEE) received the B.Eng. degree (Hons.) in electrical engineering and the M.Eng. degree in electrical power engineering from Universiti Teknologi Malaysia, in 2007 and 2010, respectively, and the Ph.D. degree in electronics and electrical engineering from the University of Southampton, U.K., in 2013. He is currently an Associate Professor with the Institute of High Voltage and High Current, Universiti Teknologi Malaysia. His current research interests include high-voltage engineering, dielectric materials, and renewable energy systems. He is a Chartered Engineer of the Engineering Council U.K., a Professional Engineer of the Board of Engineers Malaysia, and the Past Chair of the IEEE DEIS Malaysia Chapter.



WAN RAHIMAN (Member, IEEE) received the bachelor's degree in manufacturing engineering from Cardiff University, U.K., and the Ph.D. degree in fault detection and isolation for pipeline systems from the Control System Centre, University of Manchester, in 2009. Then, he became an Engineer with Panasonic Manufacturing Ltd., Cardiff, and Lotus Cars Ltd., Norwich, for several years. Currently, he is a Senior Lecturer with the School of Electrical and Electronic Engineering, Universiti Sains Malaysia (USM), Engineering Campus, Penang, Malaysia. At USM, he is also the Head of the Cluster of Smart Port and Logistic Technology (COSPALT). His current research interests include modeling nonlinear systems on a range of development research projects, particularly in drone and autonomous vehicle technologies.



ZULKURNAIN ABDUL-MALEK (Senior Member, IEEE) received the B.E. degree in electrical and computer systems from Monash University, Melbourne, Australia, in 1989, the M.Sc. degree in electrical and electromagnetic engineering with industrial applications from the University of Wales Cardiff, Cardiff, U.K., in 1995, and the Ph.D. degree in high-voltage engineering from Cardiff University, Cardiff, in 1999. He was with Universiti Teknologi Malaysia (UTM) for 30 years, where he is currently a Professor of high-voltage engineering with the Faculty of Engineering. He is also the Director of the Institute of High Voltage and High Current (IVAT), UTM. He has published two books and has authored and coauthored more than 150 papers in various technical journals and conference proceedings. His current research interests include high-voltage instrumentation, lightning protection, detection and warning systems, partial discharges, nano dielectrics, and condition monitoring of power equipment. He is a member of the MT 03 IEC 60060-2 High voltage test techniques-2: Measuring systems and the Chairperson of

the ICPADM 2021 Organizing Committee, Malaysian High Voltage Network (MyHVNet), from 2015 to 2016, and the Malaysian Working Group on High-Voltage and High-Current Test Techniques. He is also a member of the Malaysian IEC Certification Body Management Committee, the Malaysian Technical Committee on High Voltage Power Transmission, and the Department of Standards IEC 17025 Technical Assessors. He is also a member of the IEEE Power and Energy Society, the IEEE Dielectrics and Electrical Insulation Society, IET, and CIGRE. He is actively involved in many international and national committees.



SAMIR AHMED AL-GAILANI received the B.Sc. degree from the Higher Technical Institute, Aden, Yemen, in 1992, and the Ph.D. degree in optoelectronics from the University of Technology Malaysia (UTM), in 2014. He started his career as a Senior Lecturer with the Higher Technical Institute. Since then, he has been given various responsibilities, including teaching, a postdoctoral fellow, supervising laboratory sessions, supervising post-graduate students and undergraduate students, an academic advisor, the head of the laboratory, the head of the research group, the chairman, and a member of different committees and conducting short courses and training. He has authored 20 ISI articles and has an H-index of seven and a total citation of 212. He has presented more than 90 papers in reputed refereed conferences. He also successfully supervised nine undergraduate students. He received the Best Student Award for the Ph.D. degree.



SALEM MGAMMAL AL-AMERI received the B.Eng. degree in mechatronics engineering from Asia Pacific University (APU), in 2012, and the M.Eng. and Ph.D. degrees in electrical from Universiti Tun Hussein Onn Malaysia (UTHM), in 2016 and 2020, respectively. He was a Post-Doctoral at Universiti Tun Hussein Onn Malaysia UTHM and Universiti Teknologi Malaysia UTM from August 2020 to January 2023. He is currently a Lecturer with Curtin University Malaysia. His research interests include transformers Condition monitoring, High voltage, Renewable Energy, and electrical testing.

ENAS ALI received the Ph.D. degree from Mansoura University, in 2021. She is currently an Assistant Professor with the Faculty of Engineering and Technology, Future University in Egypt.



SHERIF S. M. GHONEIM (Senior Member, IEEE) received the B.Sc. and M.Sc. degrees from the Faculty of Engineering at Shoubra, Zagazig University, Egypt, in 1994 and 2000, respectively, and the Ph.D. degree in electrical power and machines from the Faculty of Engineering, Cairo University, in 2008. Since 1996, he has been teaching with the Faculty of Industrial Education, Suez Canal University, Egypt. From 2005 to 2007, he was a Guest Researcher with the Institute of Energy Transport and Storage (ETS), University of Duisburg-Essen, Germany. He is currently with the Electrical Engineering Department, Faculty of Engineering, Taif University, as an Associate Professor. His current research interests include grounding systems, dissolved gas analysis, breakdown in SF₆ gas, and AI technique applications.

...